Responsible (Name, Organisation) Massimo Ceraolo – Università Pisa	**DELIVERABLE REPORT**		Page 1(34)
Issuer (Name, Organisation) Massimo Ceraolo – Università Pisa	Date 2.5.2013	WP No 3200	Report No 3200.7
Subject Algorithm for Li cell			Dissem. Level **PU**

Deliverable 3200.7

Algorithm for Li cell

Summary

This deliverable presents a mathematical technique, and related practical algorithm, able to on-line evaluate the cell's state-of-charge (SOC) based on a cell's mathematical model (detailed in D3200.5 [1]) and on a Luenberger-style estimation that takes advantage of an Extended Kalman Filter. This work is part of WP3200 "Basic storage system testing and modelling", in Task 3230 "Modelling", with the scope to develop and validate, with experimental test work, dedicated mathematical models for Li and SC cells. As planned, the algorithm and the practical mathematical model analysed in this report are the practical exemplifications of dynamic models derived from testing activities to support the implementation of BMU (battery management unit).
This document has first put in evidence the huge difficulties for SOC evaluation of the HCV cells arising from its characteristics. The resulting algorithm mixes ampere-hour counting, OCV-SOC evaluation with our original transition model between the two stabilised OCV curves, and a Kalman filter. The algorithm effectiveness has been evaluated using a clearly defined technique. Subsequently, evaluation was made in several cases, and conditions. In all cases the algorithm recovered in reasonable time the initial errors, and remained stably very near to the "actual" and "effective" SOC value.

The algorithm has also shown "long term stability". Naturally, when the vehicle is at rest, e.g. during nights, it must be made aware of this rest, otherwise it could continuously crunch just measure errors and offsets, thus leading to unacceptable results.

Finally, the algorithm gave good results even after one year of calendar life had passed: this means that no important drift in the cell's behaviour had occurred.

In conclusion, the results of the proposed technique (and algorithm) are satisfying for practical needs and application in an HEV (hybrid electric vehicle).
.

Table of contents

List of figures

List of tables

Nomenclature

1. Acronyms

BMU Battery Management Unit
DC Direct current; design capacity
EKF Extended Kalman Filter
HCV Hybrid Commercial Vehicle
LFP lithium-iron phosphate (active chemical material for the cathode of Li cells)
Li Lithium (used in this report for indicating Lithium-ion cell design)
LTV linear time varying
OCV Open-Circuit Voltage
SOC State-of-Charge

2. Other common quantities

C electric capacitance (of the cell equivalent circuit)
C_n rated battery capacity (e.g. in Ah)
ε_i max error on current measurement *I p.u. of* I_{maxs}
ε_s max allowed error on SOC estimate
ε_Q max allowed error charge exiting the cell (Ah)
f_i current factor (ratio of maximum current to nominal current)
E_m Main-branch electromotive force
I_m Main-branch battery current
I_{maxs} maximum current the sensor can measure
I_t Cell terminals current
k transition speed of the hysteresis model
R_0 Algebraic battery internal resistance
R_i (i = 0, 1, …) i-block supercapacitor internal resistance
C_i (i = 0, 1, …) i-block supercapacitor internal capacitance
C_n Nominal capacity
U_{oc} Open-circuit voltage *(similar to OCV)*
U_{SOC} Voltage on *charge subcircuit* numerically equal to SOC

3. Quantities specific of the EKF algorithm:

$g(\ )$ function modelling hysteresis: its input is SOC, its output U_{oc}
x main state variable: numerically equal to $SOC=U_{SOC}$
y output variable; numerically equal to U_{oc}
a_{1k}, b_{1k} inner coefficients defined in equation (4)
$\sum_w$ process noise covariance
$\sum_v$ measurements noise covariance
L_k Kalman gain matrix

Introduction

In deliverable D3200.5 a detailed mathematical model of the lithium cell was illustrated and experimentally customized to the HCV Li cell with the determination of numerical parameters. The issues concerning adequate choice of the detail level of the model, as well as automated evaluation of numerical values of all the parameters defining the equivalent electrical circuit at different State of Charge (SOC) levels was discussed.

This deliverable D3200.7 describes how this model (and related simplified algorithm) can be successfully used to on-line evaluate the cell's SOC, despite of all the difficulties that characterise this cell behaviour.

Technical progress

The cell

While D3100.5 dealt with cell modelling in general, this document refers to the cell chosen for the HCV project. The basic characteristics of this cell and related standard power behaviour are reported, for completeness of the report as achieved by the manufacturer, in Table 1 and in Figure 1.

Table 1. Basic technical Li cell characteristics.

Type	LFP
Capacity (Ah)	4,4
Nominal voltage (V)	3,3
Max/min voltage (V)	3,8/1,6
Mass (kg)	0,205
Energy (Wh)	14,5
Specific Energy (Wh/kg)	70
discharge Power (W)*	550
Specific power (W/kg)	2700

These are nominal values, based on defined operating measuring conditions.
The specific power profile of Li cells used in HCV vehicles can be seen in the plot, supplied by the cell manufacturer (Figure 1).

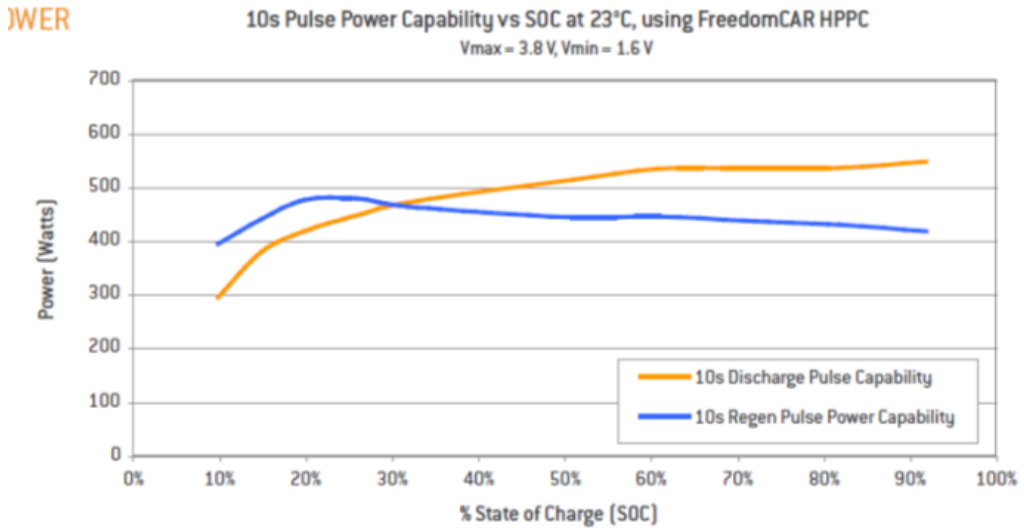

Figure 1. Charge and Discharge power as a function of SOC for the considered Li cell.

The basic difficulties

Commonly, the SOC of lithium cells is evaluated taking the integral (overall sum) of the delivered current, to obtain an Ampere-hour (Ah) counting, and correcting the values obtained in this way by means of the OCV-SOC correlation. This technique requires the measurement of OCV, when the vehicle is at rest for a sufficient time (typically half an hour), and the correction of the errors that have been accumulated during Ah counting.

However this technique cannot be conveniently used for the HCV cell, because of the simultaneous presence of three adverse factors, due to the particular chemistry of this cell and the particular operating conditions:
- high power
- OCV-SOC hysteresis
- OCV-SOC quasi-horizontal shape

These adverse factors are addressed and adequately solved in the next sections.

High power

In the past, electrochemical storage cells were not able to deliver power at the same level of the HCV Li cell.
Old lead-acid batteries, even those specifically developed for electric and hybrid vehicles, were indeed designed for maximum currents that were able to fully discharge the battery on one hour or more. Alkaline nickel-metal hydride cells, more used from the inception of the Hybrid electric vehicle market, had better power performances with respect to lead-acid batteries, but not comparable with those of HCV Li cells. Conventionally, a current that discharges an old lead-acid cell in one hour is indicated as:

$I_{max} = I_{1h}$

More recently, the first "power oriented" lithium cells allowed, especially during charge, currents that were considered very high, able to discharge the cell in half an hour or less, with an indicative maximum current:

$I_{max} = I_{0.5h} \cong 2xI_{1h}$

The HCV cells, on the other hand, can be exploited up to much higher currents. From Figure 1, considering as a hypothesis an average voltage of 2.5V during charge and of 2.5V during discharge, these currents can be estimated (10-second average, SOC=30%) to be around:

$I_{charge,max} = \cong 30\ xI_{1h}$ $I_{disch,max} = \cong 40\ xI_{1h}$

Discharge currents at SOC=30% can reach a very high peak of:

$I_{peak,30}$=470/1.6=300A= 68 x Cn

These values suggest that maximum currents of around 20-30 xI_{1h} can be safely exploited in normal practice.
This very high maximum current in comparison to the cell's capacity has strong impact on the quality (accuracy and reliability) of Ampere-hour counting with OCV-SOC correction technique.

In fact, this Ah measuring approach creates a strong limitation in the time between two OCV-SOC corrections.

To perform this analysis, it is necessary to define some symbols (Table 2).

Table 2. Symbols to evaluate accumulated error on SOC and relative description.

Symbol	*meaning*	*Description*	*Example value*
I_{maxs}		Maximum current the sensor can measure	
f_i	current factor	maximum discharge factor expressed as a ratio to the one-hour discharge current[1]	
ε_I	max current error	the maximum error the current sensor can make, as a ratio to I_{maxs}	0.01
ε_Q	max charge error	maximum error on the charge exiting the cell, as obtained by numerical integration of the measured current	-
ε_S	max SOC error	maximum allowed error on SOC estimate, before an OCV-SOC correction is needed	0.10

To evaluate the error induced on ε_Q by the errors on current measurements and subsequent numerical integration, it can be assumed that:

- time is measured with a precision that is much higher than that of current, and therefore errors on the measurement of time can be neglected;

[1] Very often the maximum discharge currents are said to be one C_n, or 2xC_n, or 5xC_n, for instance. This is formally incorrect, because currents cannot be compared with charges. In these examples, it will be 1, 2, 5 respectively, if the nominal capacity is expressed, as the maximum charge that can be delivered in one-hour discharge.

- errors in evaluation of the integral of current as a consequence of the numerical integration formulas are negligible as well.

Both assumptions are reasonable, because time is actually measured very accurately with cheap instrumentation, and numerical integration can be very precise at a very low cost using the computation power of modern microcontrollers with floating-point units.

Under these assumptions it can be written that:

$\varepsilon_{Q=}\varepsilon_{I}$x I_{maxs}xΔt

and

$$\varepsilon_s = \frac{\varepsilon_Q}{C_n} = \varepsilon_i \times f_i \times \Delta t$$

These equations very clearly show that at equal ε_I and ε_s, the maximum time, for which the Ah-counting can proceed before OCV-SOC correction, depends on f_i.

Considering the exemplified values for the maximum errors shown in Table 3, values of Δt for a conventional lithium battery and the HCV cell are reported in the last column of the same table.

Table 3. Values of Δt using example data.

Cell	f_i	ε_i	ε_s	Computed Δt/h
Conventional lithium	1	0.01	0.1	10
HCV cell	30	0.01	0.1	0.33

It is therefore confirmed, that even in case the cell had a manageable OCV-SOC correlation waveform (no hysteresis, no quasi-horizontal parts), the technique for estimation of SOC by combined Ah-counting and OCV-SOC correlation is hardly feasible, because its OSV-SOC correlation can be done only when the vehicle is at rest for at least half an hour.

Hysteretic and quasi-horizontal OCV-SOC correlation

In deliverable D3200.5 [1] the experimental result on OCV was shown (in Figure 17 of that deliverable that is replicated here for the reader's convenience in Figure 2), with indication of the experimental points and spline interpolation.

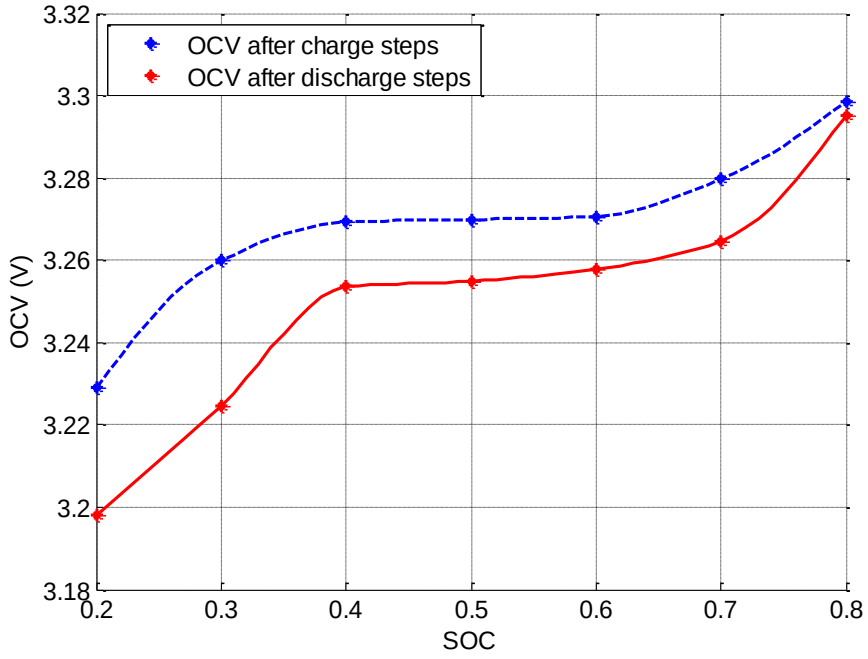

Figure 2. Cell U_{oc} after discharge steps and charge steps: experimental data (crosses) and spline interpolation.

Figure 2 clearly shows two issues:

- a large quasi-horizontal part in the central SOC zone;
- a marked variation in the OCVs after charge steps and discharge steps.

This does not allow evaluating SOC by a simple measurement of OCV.
The solution that has been found for the HCV project is to evaluate SOC based on all the dynamic behaviours of the cell, by comparing the model and measured voltages.

Including hysteresis in the cell's mathematical model

The final, called "form 2", representation of the cell's mathematical model is shown in Figure 4 of deliverable D3200.5, that is replicated here, as Figure 3, for the reader's convenience.

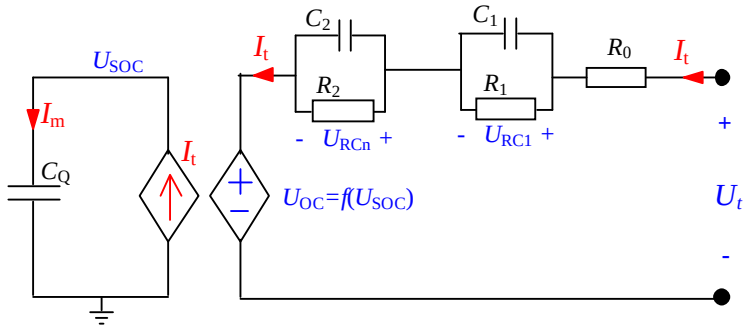

Figure 3. Cell model with 2 R-C blocks (form 2).

Remember that according to this modelling U_{SOC} is a voltage value in the left subcircuit. (called *charge subcircuit*). Its numerical value is equal to what is normally indicated as SOC:

U_{SOC}=SOC.

The key to a good mathematical hysteresis model lies in trying to emulate the hysteresis in the OCV behaviour not only when the electrochemical cell traverses the major loops (0 to 100% SOC) but also during minor loops (small charge-discharge cycles during a larger overall charge or discharge).
Indeed for hybrid vehicles in general, and for HCV vehicles in particular, the SOC variation window during normal operation will be much smaller than the full potential SOC range.

The basic idea is to try to create a mathematical model that tends to move U_{oc} towards the upper curve when the cell is charging and towards the lower one when it discharges. The speed of this transition needs to be evaluated based on cell tests.

In pursuing this objective, after some attempts the following mathematical formulation has been proposed, which determines the derivative of U_{oc} as a function of the direction in which SOC is moving, and on how far actual model U_{oc} is from the target curve.
The target curve is the upper curve (blue in Figure 2) when the cell is charging, the red one when it is discharging.

$$\frac{dU_{oc}(U_{SOC})}{dU_{SOC}} = \begin{cases} \frac{dU_{OCch}(U_{SOC})}{dU_{SOC}} + k(U_{OCch}(U_{SOC}) - U_{OC}(U_{SOC}), & \frac{dU_{SOC}}{dt} \geq 0 \\ \frac{dU_{OCdisch}(U_{SOC})}{dU_{SOC}} - k(U_{OCdisch}(U_{SOC}) - U_{OC}(U_{SOC}), & \frac{dU_{SOC}}{dt} < 0 \end{cases} \quad (1)$$

The algorithm works as follows:

- when the time-derivative of U_{oc} is positive, the model U_{OC} is gradually moved towards U_{OCch}, (the blue curve in Figure 2) using a derivative that is the corresponding target derivative $\frac{dU_{OCch}(U_{SOC})}{dU_{SOC}}$ plus a correction factor $k(U_{OCch}(U_{SOC}) - U_{OC}(U_{SOC})$

- when the time-derivative of U_{oc} is negative, the model U_{OC} is gradually moved towards $U_{OCdisch}$, (the red curve in Figure 2) using a derivative that is the corresponding target derivative $\frac{dU_{OCdisch}(U_{SOC})}{dU_{SOC}}$ plus a correction factor $-k(U_{OCdisch}(U_{SOC})-U_{OC}(U_{SOC})$

Therefore, the dimensionless parameter *k* determines the speed of transition from one curve to the other, and therefore is called *transition speed* of the algorithm.
To better understand how this algorithm actually works, a test case has been prepared, which refers to the somewhat idealized voltage behaviour shown in Figure 4.

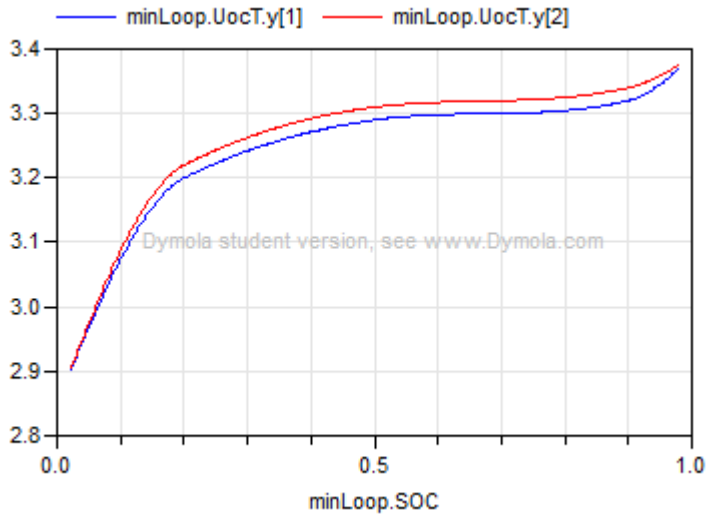

Figure 4. An idealized hysteretic OCV-SOC curve for algorithm testing.

The algorithm is tested submitting the algorithm (1) to an input SOC that is sinusoidally varied between two limits. For instance the result between SOC=0.2 and SOC=0.4, using a value of k=10 is shown in Figure 5.

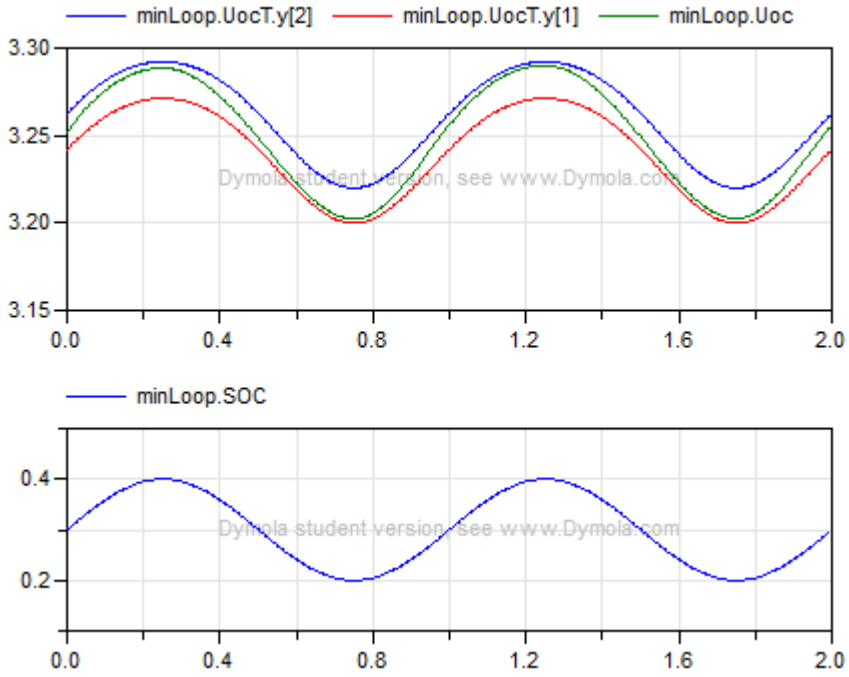

Figure 5. Effect of algorithm (1) in case of k=10, in a sample case.

Figure 5 clearly shows that when SOC increases, the model UOC (named minLoop.Uoc in figure where it is represented in green) tends to approach the upper U_{oc} bound (blue in figure), while, when SOC decreases, it tends to approach the lower bound.

The effect can be made more marked raising the speed of transition between curves, defined by factor *k*. For instance the result with *k*=30 is that shown in Figure 6.

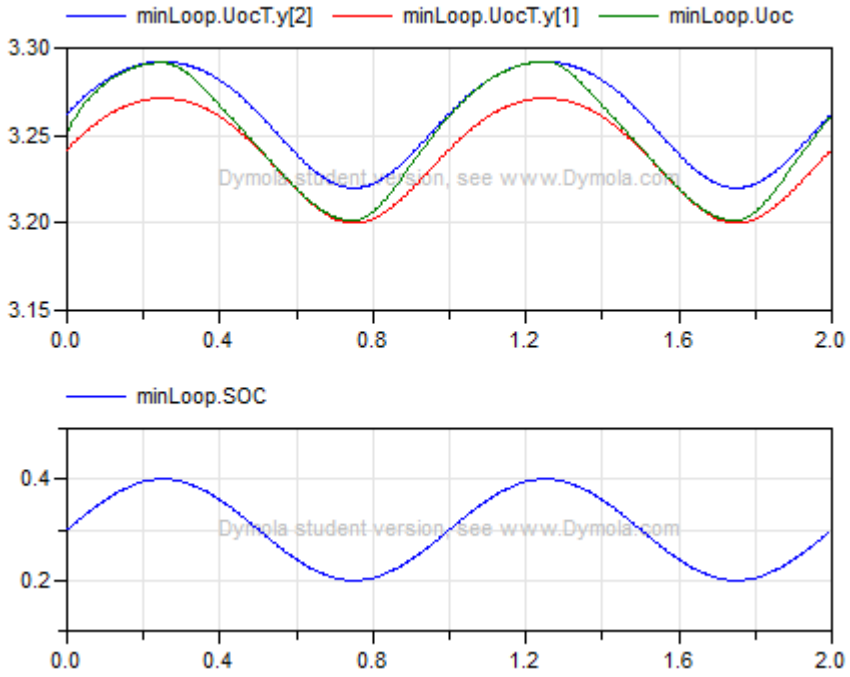

Figure 6. Effect of algorithm (1) in case of k=30, in a sample case.

The value for the transition speed for a given cell can be determined using a specific test.

The value that has resulted to be adequate for the HCV cell is *k*=13.

It must be noted that the algorithm is robust, since it recovers initial errors fast. This is clarified in Figure 7. At the starting time, the initial estimate of U_{oc}, which in the previous examples was the arithmetic mean between the corresponding values of the two target curves, gives an offset of 0.05. It is seen that, during SOC swings, the algorithm rapidly recovers, and U_{oc} enters the stripe defined between the two target curves.

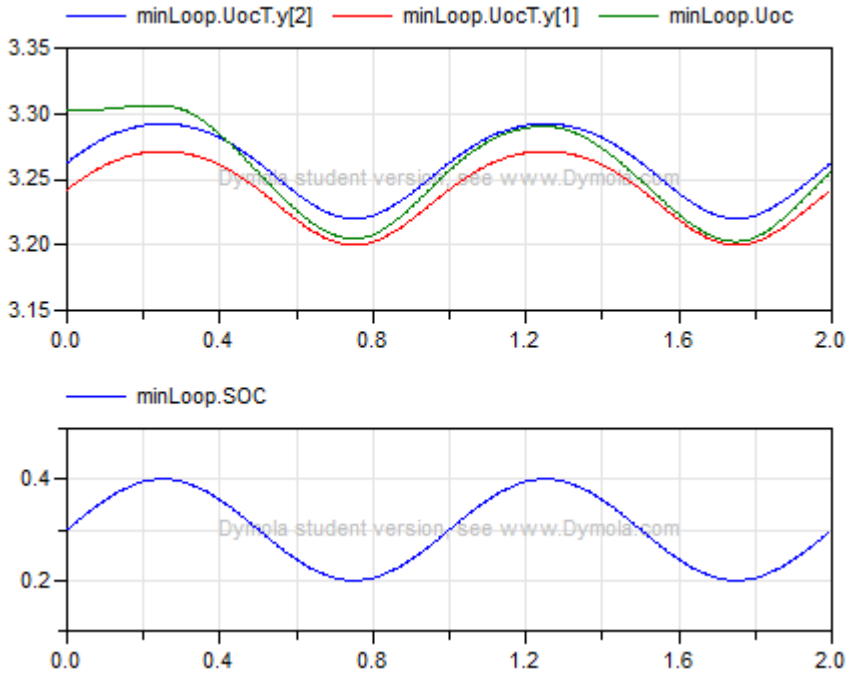

Figure 7. Recovery of algorithm (1) from an initial error (k=10).

According to the agreements among HCV partners, tests were performed using the so-called Altra cycle, which was defined in terms of battery power. That cycle has been scaled down to a cell level, and considered as being a current cycle instead of a power cycle, since cell tests are much more easily made in terms of current.
The result is that illustrated in Figure 8. Currents are positive when charging. The profile is composed by a sequence of segments of straight line; the corner points are indicated by square markers.
This cycle is based on Altra technical specifications and simulates the ordinary vehicle operation, .In this cycle, a power contribution is coming from the internal combustion engine, in order to balance the overall cell charge (the integral of the current is zero).

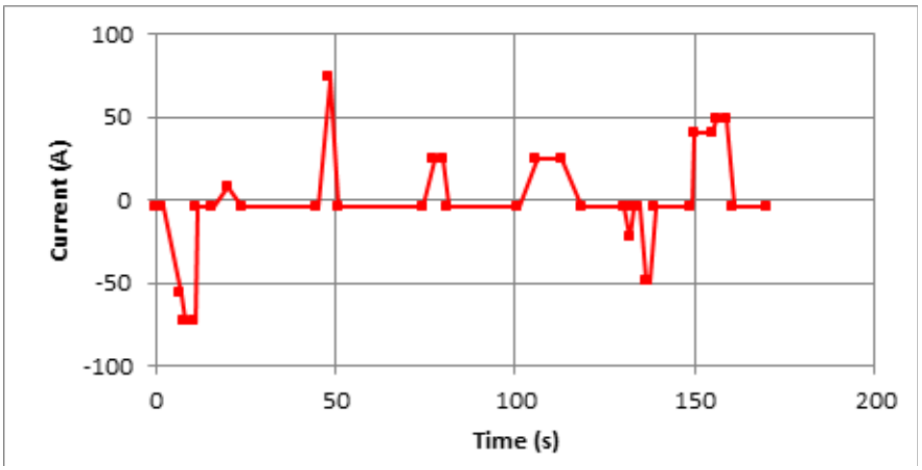

Figure 8. The "Altra" cycle reported at a cell level (positive currents indicate charging).

The corresponding charge accumulated in the battery, as obtainable by integrating the profile in Figure 8, is shown in Figure 9.

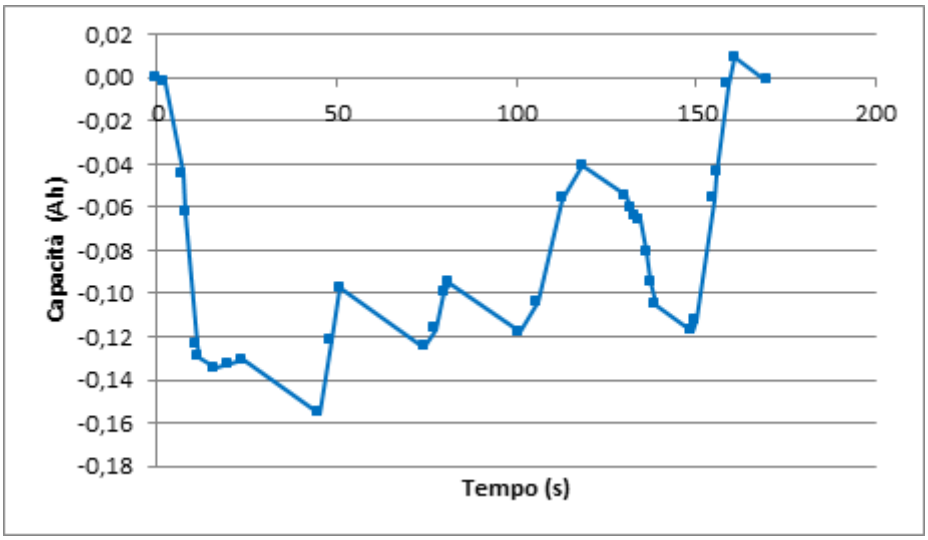

Figure 9. Charge stored in the cell when operated with current shown in Figure 8.

Algorithm (1) can be used to determine actual U_{oc} to be considered when simulating the cell model of Figure 3, taking into account the target U_{oc} curves in Figure 2, and applying to the cell the current profile of Figure 8.

The basic result is shown in Figure 10, in which at the start of simulation, U_{oc} is taken as the arithmetic mean of the two corresponding target values.

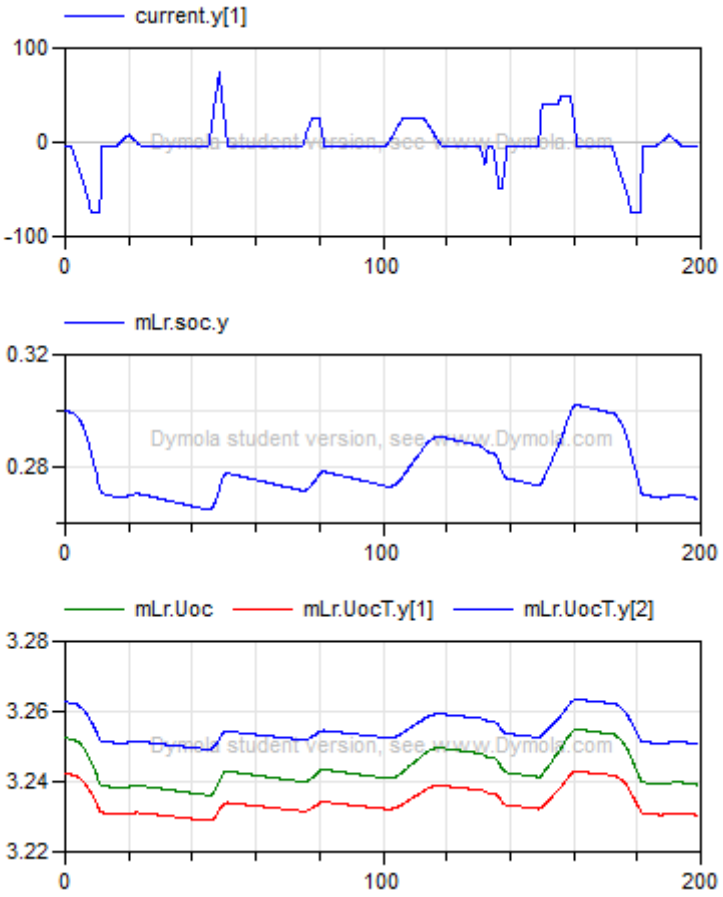

Figure 10. Application of algorithm (1) to the cell subjected to the Altra cycle (Fig. 8). Top: current; Center: SOC (starting from 0.3); Bottom: Computed (green) and target Uoc's.

Figure 10 shows that the SOC swing is so small that the actual U_{oc} stays stably inside the band, basically around the arithmetic mean.

Therefore in the software to be introduced in the vehicle, in principle the inclusion of algorithm (1) is not needed, and the arithmetic mean of the two target values can be used constantly; however, the inclusion of that algorithm allows to better determine U_{oc}, in cases the vehicle operation, for some reasons, has larger SOC swings.
A verification of the stability of the algorithm is checked in Figure 11, in which an initial offset is added to U_{oc}, and it is seen that this offset is rapidly absorbed and in a short time the evaluated U_{oc} is again the one obtained in the plots of Figure 10.

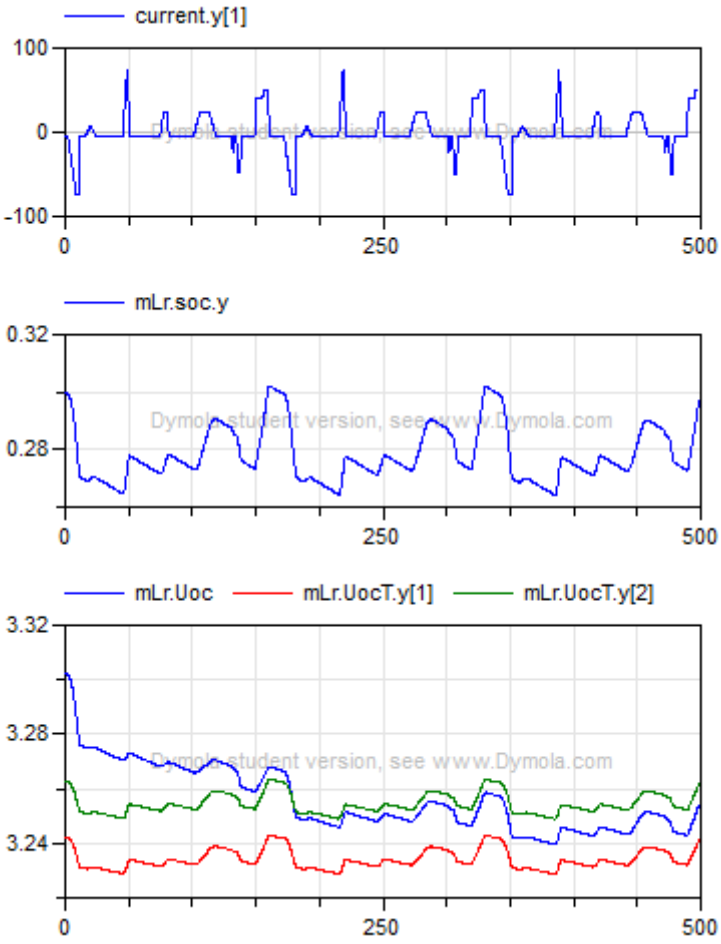

Figure 11. Application of algorithm (1) to the cell subjected to the Altra cycle (fig. 8) and adding an initial offset to U_{ov} of 0.05 V. Variables as per Figure 10.

For evaluating the effect of the algorithm (1) in case of the Altra cycle, a current swing is superposed and can be analysed looking at Figure 12, in which the current cycle of Figure 8 is modified, by adding 100A for the first 120s, and by subtracting 100 A between *t*=120s and t=240s.

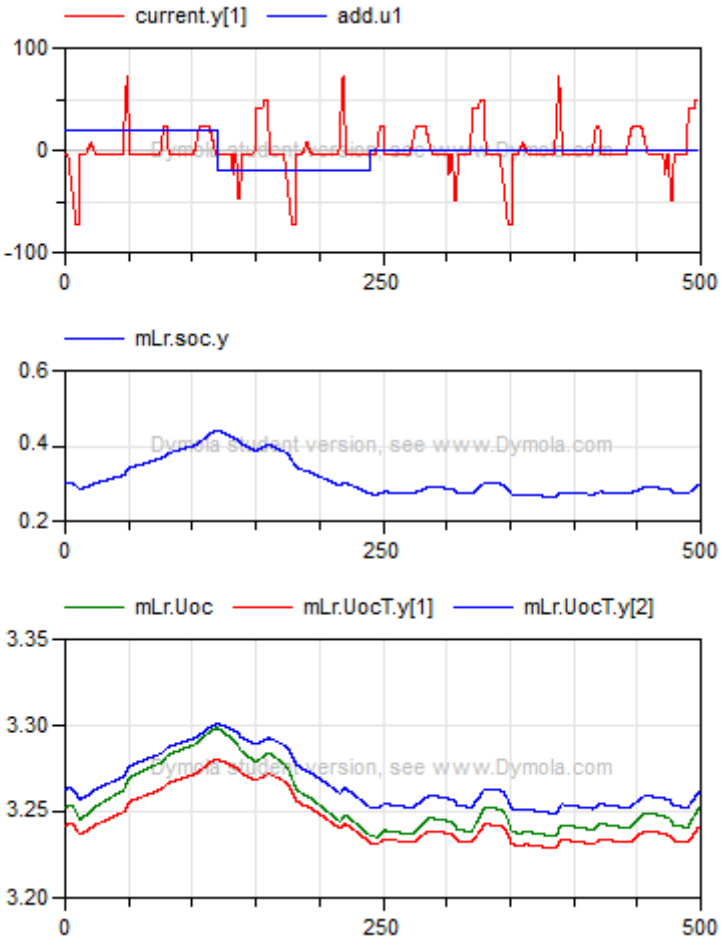

Figure 12. U_{oc} evaluation with the Altra current cycle with superposition of a larger current causing SOC swing. Actual current: the sum of the two terms shown in the top plot.

Figure 12 clearly shows that, during the first SOC rise, the computed U_{oc} moves towards the higher target, i.e. the discharge OCV target, when SOC falls, the computed U_{oc} tends to the lower target; finally, when the current balance is restored, U_{oc} gets back in the centre of the stripe.

Algorithm to estimate the battery's SOC

In the previous sections discussion has been made about the difficulties of the most common ways to estimate cell SOC:

1) Ah-counting creates accumulated errors that, for the high power cells such as the HCV's can reach 10% in as small time as 20 minutes. Therefore this technique can be used only for very short times;
2) OCV-SOC correlation brings the additional difficulty that, for the central SOC zone, OCV is nearly horizontal, and that there is a marked hysteresis phenomenon that further complicates the analysis.

To try to obtain as accurate as possible SOC evaluation it is deemed that all the available techniques and information should be simultaneously exploited.

Consequently, the basic idea that was issued is to cycle between Ah-counting and OCV estimation, to compensate errors. The algorithm's basic arrangement can therefore be as shown in Figure 13.

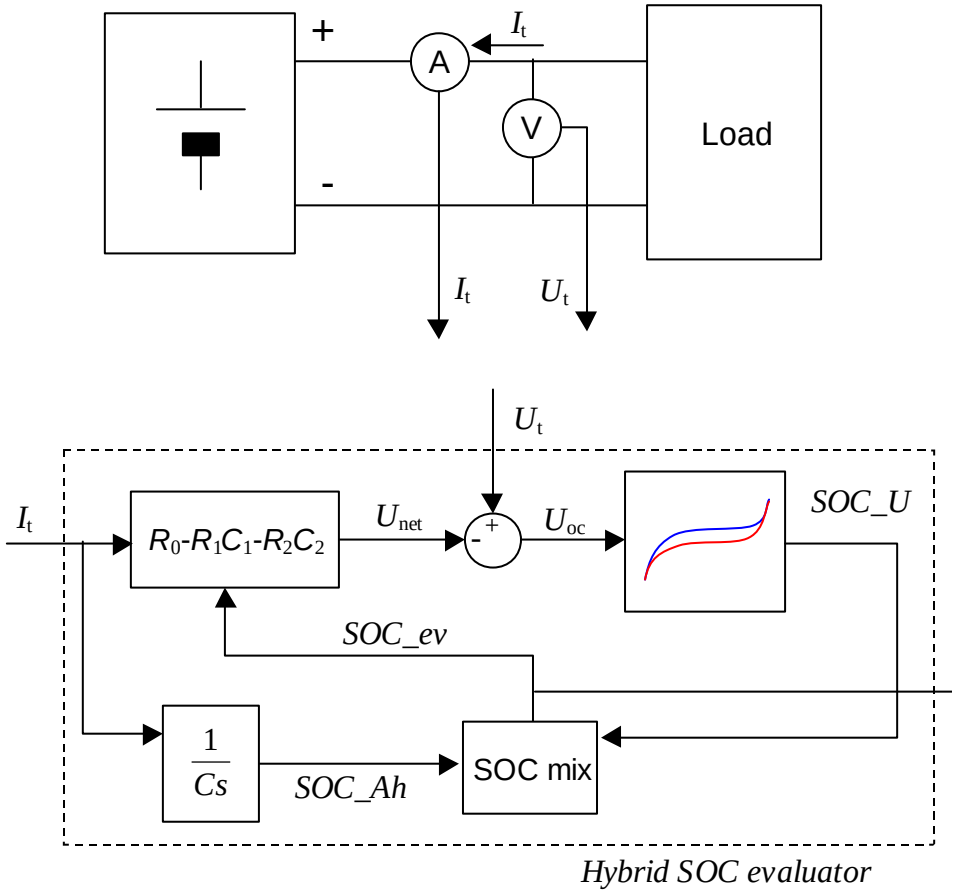

Figure 13. Hybrid SOC evaluator, basic concept.

Measurements of cell's voltage and current are taken from the physical system, as shown in the upper part of Figure 13.
These two measurements are fed into the Hybrid SOC evaluator, which then gives the output.

The evaluator operates in two directions:

- In the upper chain it makes a voltage-based SOC evaluation: from the measured cell's terminal voltage U_m, determines the circuit U_{oc} (by subtraction of the voltage drop across the electric network R_0, R_1C_1, R_2C_2) and then, using the above discussed SOC-OCV correlation, determines a SOC estimation.
- In the block containing 1/(Cs) ("in which "s" is the Laplace variable) another SOC estimation is obtained, based on ampere-hour counting.

The two SOC evaluations must then be somehow mixed to determine the final estimate SOC_ev.

In addition to the technique depicted in Figure 13, adequate treatment of measuring errors must be made, for instance by taking advantage of Kalman filters.

After some attempts, the final implementation of the basic logic concept presented in Figure 13, which showed good estimation quality, is represented in Figure 14 (where the upper part of Figure 13 is omitted for the sake of simplicity).

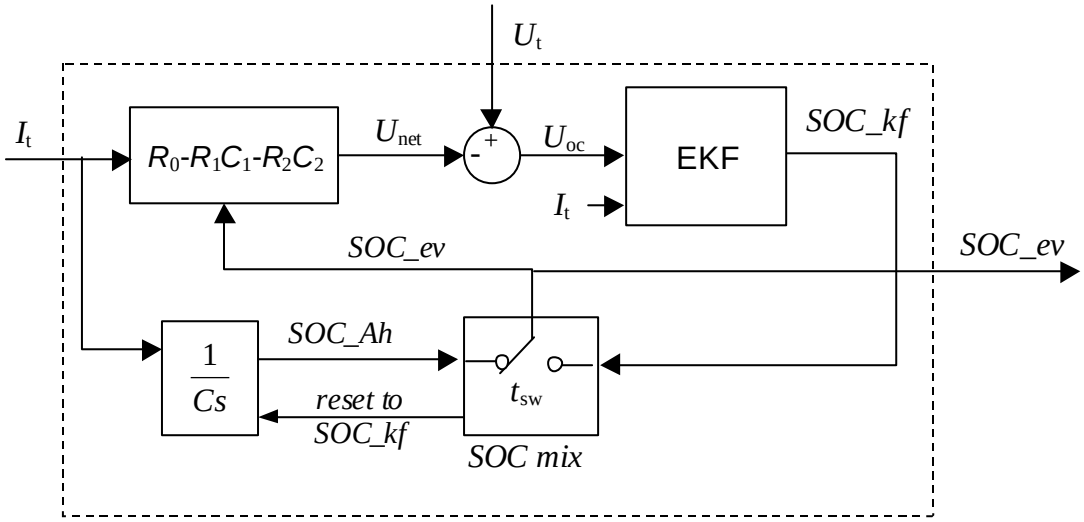

Figure 14. Hybrid SOC evaluator, actual implementation.

In comparison to Figure 13, the following differences have been introduced:

- Instead of a simple hysteresis block, a full Extended Kalman filter (EKF) has been introduced that performs SOC_U evaluation taking also into account the measured current I_m, and adequately treating measurement errors.
- The "mix" block was chosen as a switch that periodically resets the value of SOC_Ah: normally is SOC_ev=SOC_Ah; however periodically it is forced to be SOC_*ev*=SOC_*kf*, and the integral 1/(Cs) is reset to accommodate for this new output value.

In section "High power" above it was seen that for high power cells such as the ones used for HCV project Ah-counting leads to errors on SOC of about 10% after 20 minutes. Therefore the periodicity of the mix block must be lower than this value.
Several simulations were performed on this time, and it was seen that values between 1-10 minutes give the best results. Therefore, it was assumed, for the final simulations performed, and reported below that t_{sw}=5 min.

The R-RC-RC Network: details

The set of equations (2) describe the dynamic behaviour of the system represented in Figure 3.

$$\frac{dU_{OC}(U_{SOC})}{dU_{SOC}} = \begin{cases} \frac{dU_{SOC}}{dt} = -\frac{U_{SOC}}{R_{sd}C_q} + \frac{I_t}{C_q} \\ \frac{dU_{RC_1}}{dt} = -\frac{U_{RC_1}}{R_1C_1} + \frac{I_t}{C_1} \\ \frac{dU_{RC_2}}{dt} = -\frac{U_{RC_2}}{R_2C_2} + \frac{I_t}{C_2} \\ U_t = U_{oc} + R_0 I_t + U_{RC_1} + U_{RC_2} \end{cases} \quad (2)$$

The discrete form of these battery transient equations can be expressed as follows:

$$\begin{cases} \boldsymbol{x}_{k+1} = \boldsymbol{A}\boldsymbol{x}_k + \boldsymbol{B}\boldsymbol{u}_k \\ \boldsymbol{y}_k = \boldsymbol{C}\boldsymbol{x}_k + \boldsymbol{D}\boldsymbol{u}_k \end{cases} \qquad \begin{cases} \boldsymbol{u} = [I_t] & \boldsymbol{x} = [U_{RC1} \quad U_{RC2}]^T & \boldsymbol{y} = [U_t - U_{oc}] \\ \boldsymbol{A} = \begin{bmatrix} e^{-t/R_1C_1} & \\ & e^{-t/R_2C_2} \end{bmatrix}; & \boldsymbol{B} = \begin{bmatrix} R_1\left(1-e^{-t/R_1C_1}\right) \\ R_2\left(1-e^{-t/R_2C_2}\right) \end{bmatrix} \\ \boldsymbol{C} = [1 \quad 1]^T & \boldsymbol{D} = R_0 \end{cases} \quad (3)$$

where R_0, R_1, R_2, C_1 and C_2 are the cell parameters as a function of SOC and thus indirectly varying with time.

The vector of state variables ***x*** is constituted by the two voltages across *R-C* blocks.
As usual, matrix ***A*** represents the dynamic evolution of state ***x***, matrix ***B*** indicates the quota of input directly transferred to states (algebraic part of *R-C* blocks) and matrices ***C*** and ***D*** indicate the influence of state and input into output, constituted by the battery's voltage at its terminals.

The Extended Kalman filter (EKF) block: details

The Extended Kalman filter technique is applied to the dynamic system 3 that describes the transient behaviour of the left part of the electrical circuit illustrated in Figure 3:

$$\frac{dU_{SOC}}{dt} = -\frac{U_{SOC}}{R_{sd}C_q} + \frac{I_t}{C_q} \quad (4)$$

The EKF uses the measured current (I_t) and the OCV (obtained as the difference between the output of the R-RC-RC Network block and the voltage measurements) to perform the runtime SOC evaluation.
The detailed equations of this block are as follows:

$$\begin{cases} x_{k+1} = f(x_k, u_k) + w_k = a_{1_k}x_k + b_{1_k}u_k + w_k \\ y_k = g(x_k) + v_k \\ x = U_{SOC} \\ u_k = I_t \\ y = U_{OC} \\ a_{1_k} = e^{\frac{-t_k}{R_{sd}C_Q}} \\ b_{1_k} = R_{sd}\left(1 - e^{\frac{-t_k}{R_{sd}C_Q}}\right) \end{cases} \quad (5)$$

Note that $g(\cdot)$ is the U_{SOC} - U_{OC} correlation function, which is able to take into account voltage hysteresis, according to the analysis performed in section "Including hysteresis in the cell's mathematical model" above and summarized by equations (1).
Moreover, w_k and v_k are the process and the measurement noises, respectively. They are assumed to be independent to each other and with white normal distributions with a zero mean and covariance of known values.
State estimate time update can be expressed as:

$$\hat{x}_k^- = \hat{A}_{k-1}\hat{x}_{k-1}^+ + B_{k-1}u_{k-1} = a_{1_{k-1}}\hat{x}_{k-1}^+ + b_{1_{k-1}}u_{k-1} \quad (6)$$

where a_{1k} and b_{1k} are expressed in (5), a_{1k} is also defined as:

$$\hat{A}_k = \left.\frac{\partial f(x_k, u_k)}{\partial x_k}\right|_{x_k=\hat{x}_k^+} = a_{1_k} \quad (7)$$

The error covariance time update can be expressed as:

$$p_{\tilde{x},k}{}^- = \sum_{\tilde{x},k}^- = a_{1_{k-1}}{}^2 p_{\tilde{x},k-1}{}^+ + \sum_w \quad (8)$$

where $p_{\tilde{x},k}{}^-$ is the element of the error covariance matrix and $\sum_w$ is a constant value that represents the process noise covariance.
Considering the Jacobian $\hat{C}_k$:

$$\hat{C}_k = \left.\frac{\partial g(x_k, u_k)}{\partial x_k}\right|_{x_k=\hat{x}_k^-} = c_k \quad (9)$$

where c_k is the element of the $\hat{C}_k$, the Kalman gain matrix defined in Appendix (equation A18) could be expressed as:

$$l_k = P_{\tilde{x},k}{}^- c_k [c_k{}^2 P_{\tilde{x},k}{}^- + \sum_v]^{-1} \quad (10)$$

where l_k is the element of L_k and $\sum_v$ is a constant value that represents the measurements noise covariance.
Equation (11) defines the state estimate measurement update:

$$\hat{x}_k^+ = \hat{x}_k^- + l_k[y_k - g(\hat{x}_k^-, u_k)] \quad (11)$$

The updated estimate covariance is expressed as follows:

$$l_{\tilde{x},k}{}^+ = (1 - l_k c_k) p_{\tilde{x},k}{}^- \quad (12)$$

The SOC mix block: details

As described above, every time interval t_{sw} (five minutes in the actual implementation) the block takes as SOC_ev the value coming from the EKF block, and resets the Ah-counting integral:

$$SOC = SOC_0 + \frac{1}{C_{batt}} \int_{t=0}^{t=t_{sw}} I_t(t) dt \quad (13)$$

SOC_0 is the initial SOC. At the beginning of the simulation this is a known imposed value; every five minutes this value is set to the SOC_kf.
C_{batt} is the cell's capacity.

Results and Discussion

Test definition

The quality of the EKF SOC estimation applied to the cell was tested on two main reference cycles, derived from a reference HEV cycle studied at Pisa University for validating models (Cycle 1) and from the recommended Altra cycle for HCV commercial van. The two cycles, corresponding to the real usage of the battery on-board hybrid vehicles, are shown in Figure 15 and Figure 16. Currents are negative when the battery is delivering power, positive otherwise. Both of the cycles were scaled at cell level, and charge compensation was introduced.

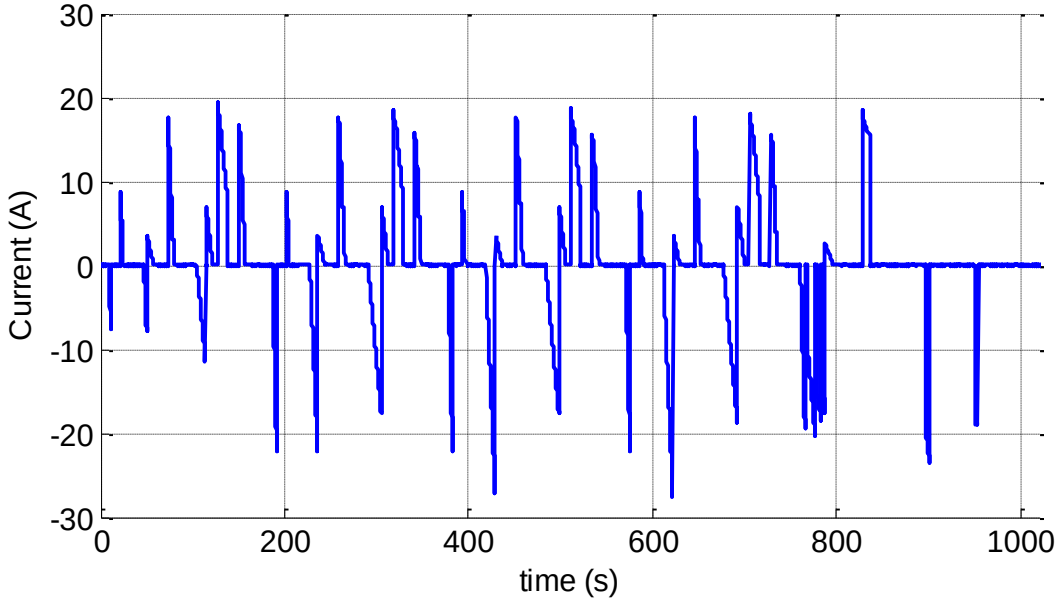

Figure 15. Cycle 1 scaled for the battery cell (Pisa University in-house cycle for model validation).

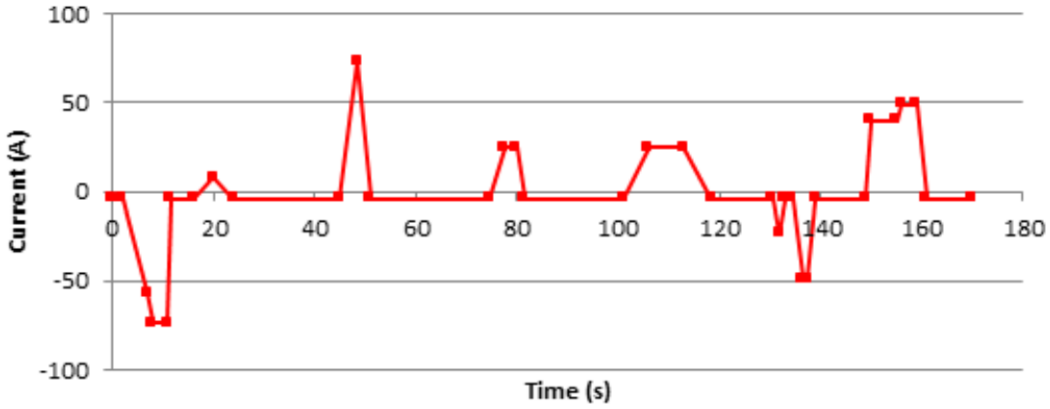

Figure 16. Cycle 2 scaled for the battery cell (from Altra HCV cycle).

The test has been executed by the repetition of several cycles and by performing the SOC evaluation through the EKF algorithm.
The initial model verification was done with Cycle 1 sequences (repeated rest and cycling: in total 18 cycles with in between a 10 min rest for a complete test sequence of 8 hours). Afterward, Cycle 2 tests were carried out with a defined procedure. The entire test lasts about 45 hours and is divided in three parts: a first sequence of 48 cycles, lasting about 5 hours, a second phase of rest (35 hours) and the second sequence of 48 cycles (5 hours). As for the previous case, results are related to the first part of the test, while some comments about long-term stability are reported later.

LFP cell: results

The test was applied on the LFP cell with reference to the Cycle 1. The cell was subjected to the current profile, and then the EKF-SOC estimator was applied.
The "true" SOC was obtained by numerical integration of current, measured with very precise lab instrumentation, and the parameters[2] of RC network were determined as a function of SOC, then the SOC estimation was performed with the EKF algorithm. Finally, the estimation of the SOC has been compared to the measured value.
It must also be noticed that the proposed algorithm should be able to be implemented onboard real buses, using commercial, inexpensive measuring hardware. To show how the algorithm is able to perform when fed with measurements from inexpensive sensors, the voltage and current data supplied to it were altered with respect to the high precision values measured with lab-grade instrumentation (the laboratory instruments had errors at the end of their scale of 0.06 % for current at 150 A and 0.035 % for voltage at 200 V), as follows:

$$I_{EKF} / A = 1{,}03\, I_{LAB}(t) + 0{,}2$$
$$V_{EKF} / A = 1{,}02\, I_{LAB}(t) + 0{,}04 \qquad (14)$$

I.e., a 200 mA offset and 3 % error was introduced onto the current, and a 40 mV offset and 2 % error was added to voltage. Moreover, the initial SOC was set at 70 %, although the real initial SOC of the cell was about 50 %.
The test lasts 45 hours. Figure 17 shows results related to the first part of the test, while some comments about long-term stability are reported later. The estimated *SOC* by the EKF algorithm (red curve) matches the *SOC* obtained by the numerical integration of the experimental measured current (blue curve), recovering the initial error in a few hours.

[2] Details about parameters identification are reported in D3200.5

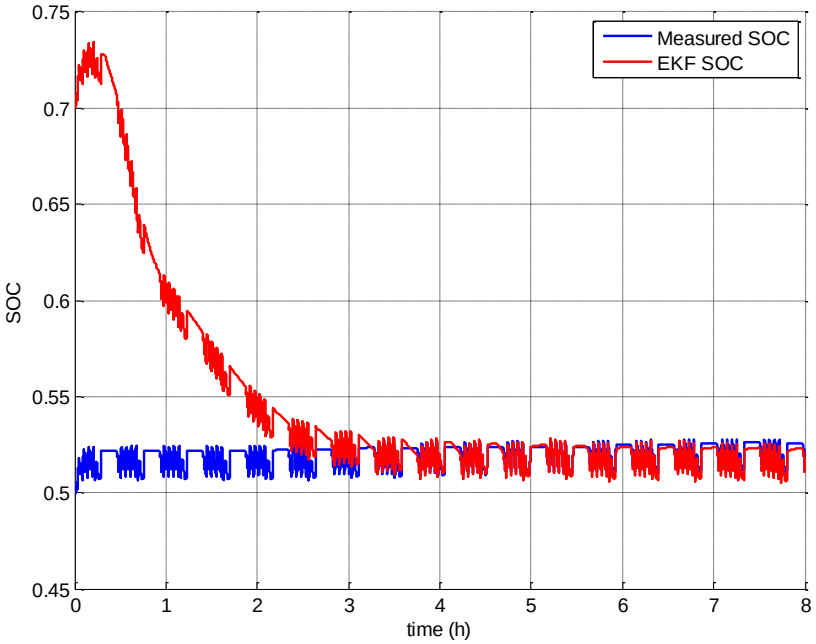

Figure 17. Experimental evaluation of battery SOC estimation using the EKF-based model for Cycle 1.

LFP aged cell: results

After the tests described in the previous section, the cell had one year rest; after this period, Cycle 2 was applied to the aged Li-ion cell, used in the HCV project.

At first level, to evaluate the stability of the algorithm, no modification of the electrical parameters (R_0, R_1, R_2, C_1, C_2) was applied. At the same, also the EKF covariances $\sum_v$ and $\sum_w$ were kept unmodified. If $\sum_v$ decreases, the evaluated VOC coming from measurements and the R-RC-RC Network, has more influence in the SOC evaluation, than the integration of the measured current. If, on the other hand, $\sum_w$ decreases, SOC estimation is more affected by the integration of the measured current than the evaluated VOC.

These covariances are tuned off-line for each set of electrical parameters (R_0, R_1, R_2, C_1, C_2) related to a specific cell.

The estimated *SOC* (red curve) matched the *SOC* obtained by the numerical integration of the measured current (blue curve) as visible in Figure 17, recovering the initial error in the same time as in the previous test (Figure 16).

This aspect is representative of the high level of stability and reliability of the proposed algorithm, able to work properly also without redefinition of the parameters.

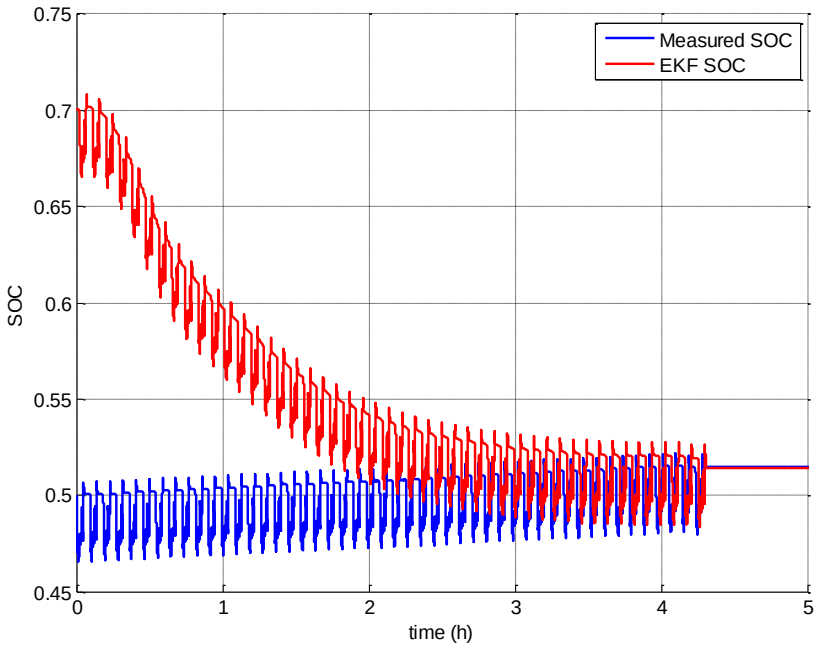

Figure 18. Experimental evaluation of battery SOC estimation using the EKF-based model, applied to an aged cell, for ALTRA road cycle.

The second test was oriented to evaluate the algorithm through a re-calibration of the electrical and the EKF parameters: particularly, a new set of electrical parameters (R_0, R_1, R_2, C_1, C_2) and the *SOC-OCV* correlation curve have been estimated. In this case, providing the same voltage and current errors (equation 14) to the experimental data, the results carried out by the EKF algorithm are less accurate than the ones showed in Figure 18 In order to have the same behaviour of the *SOC* based on EKF, also the algorithm parameters (Q and R) were changed, so that the measured VOC have less weight than the model in SOC estimation. Final result is reported in Figure 19.
This aspect shows how the re-calibration of the electrical parameters must be necessarily accompanied with the update of the EKF algorithm parameters, to maintain a good quality on the SOC estimation.

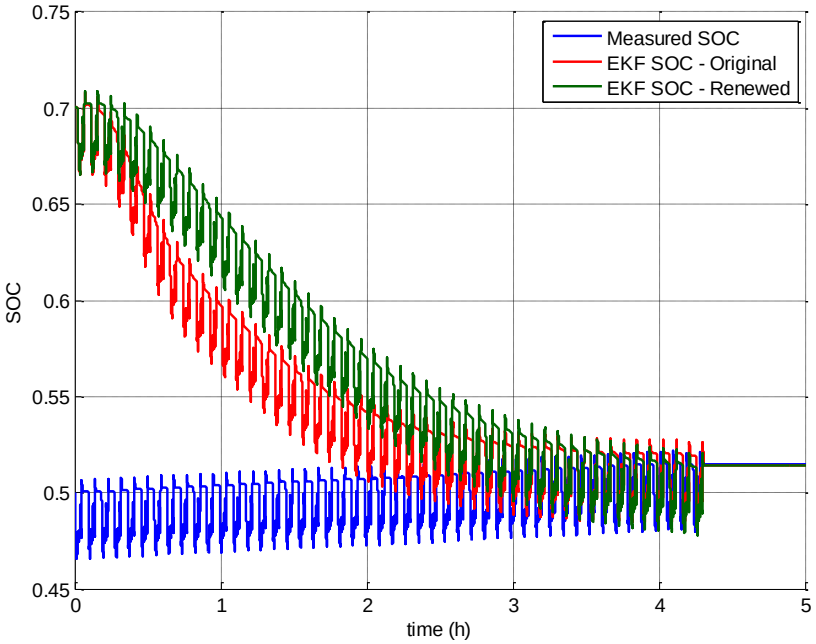

Figure 19. Comparison between EKF results obtained both for the aged cell with original (red) and renewed (green) set of electrical and parameters.

Long term stability

The long term stability for the EKF algorithm has been analysed in reference to the three case studies already presented before. More in detail, it is possible to observe that results already mentioned for the LFP cell, subjected to the Cycle 1, showed the stability of the algorithm for the total duration of the test, of about 45 hours. Results are reported in Figure 20.

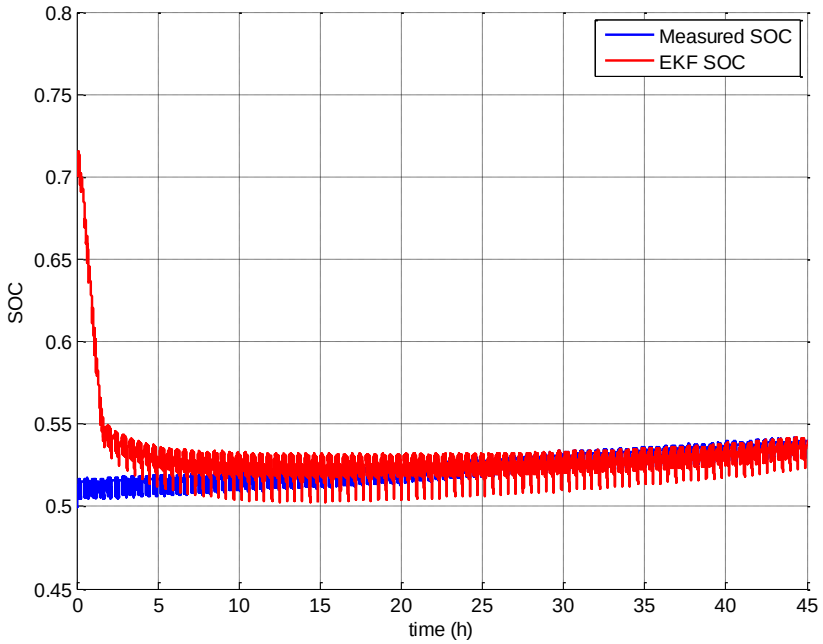

Figure 20. Experimental validation of the EKF-based model on the Cycle 1 (red: EKF estimator; blue: measured value).

Similar results were obtained for the aged cell subjected to Cycle 2 without any electrical or EKF parameters redefinition. It must be also noticed that contrary to the previous analysis, the SOC evaluation was stopped during the rest phase of the vehicle; also in this case the stability seems to be guaranteed. Redefining the electrical and the EKF parameters for the aged cell, the evaluated SOC matches accurately the SOC measured through laboratory instruments, as reported in Figure 21.

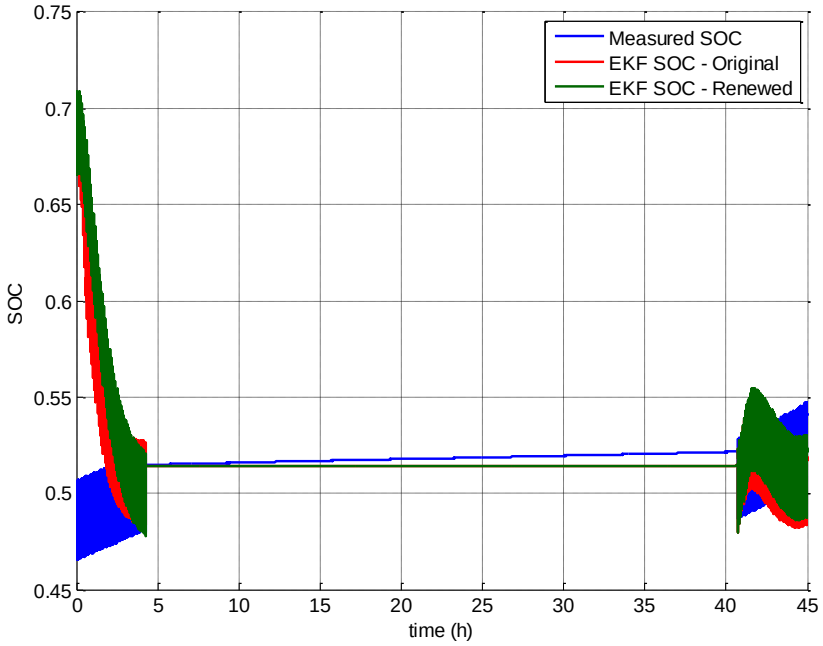

Figure 21. Experimental validation of the EKF-based model on the Cycle 2 (blue: EKF estimator; green: measured value).

Conclusions

This document has first put in evidence the huge difficulties for SOC evaluation of the HCV Li cells arising from its characteristics:

- High power, that enlarges accumulation effect of measurement errors on the ampere-hour counting
- Flat OCV-SOC curve for ample ranges of SOC, that causes difficulties in evaluating SOC from open-circuit voltage measurements
- Hysteresis on the OCV-SOC curve correlation.

These difficulties are dealt with as follows:

- The voltage hysteresis has been modelled by an original technique; transition between charge-based and discharge-based curves has a higher derivative, than the stabilized OCV curves, that eases SOC evaluation
- Adequate treatment of measuring errors was done using an Enhanced Kalman Filter.

The resulting algorithm mixes Ah-counting, OCV-SOC evaluation with our original transition model between the two stabilised OCV curves), and a Kalman filter (an EKF version).

The algorithm effectiveness has been evaluated using the following technique:

- Measurements were taken from lab tests with the highest accuracy
- The integral of these high accuracy currents was taken as the best estimate of cell SOC.

- Our algorithm has been fed with data that were altered so that it "sees" measurements that simulate values that could be taken from cheap, industrial sensors. Moreover a wrong initial SOC estimate was supplied to it.

Evaluation was made in several cases, and conditions. In all cases the algorithm recovered in reasonable time the initial errors, and remained stably very near to the "actual" SOC value.

The algorithm has also shown "long term stability". Naturally, when the vehicle is at rest, e.g. during nights, it must be made aware of this rest, otherwise it could continuously crunch just measure errors and offsets, thus leading to unacceptable results.

Finally, the algorithm gave good results even after one year of calendar life had passed: this means that no important drift in the cell's behaviour had occurred.
However, it is recommended that, when the cells and batteries are used on board production vehicles, yearly recalibration is made, to keep the algorithm in touch with the actual state of life of cell and battery. More on this point will be discussed when data on aged cells will be available for analysis, for model validation and algorithm optimization.

References

1. Hybrid Commercial Vehicle (HCV) FP7-Project, "Preliminary model definition for Li cell, D3200.5," University of Pisa, 2013.
2. Hybrid Commercial Vehicle (HCV) FP7-Project, "Modelling Test Matrices for Li batteries and SC, D3100.5," University of Pisa, 2012.
3. G. L. Plett, "Extended Kalman filtering for battery management systems of LiPB-based HEV battery packs. Part 1. Background," *J. Power Sources*, vol. 134, pp. 252-261, 2004.
4. G. L. Plett, "Extended Kalman filtering for battery management systems of LiPB-based HEV battery packs. Part 2. Modeling and identification," *J. Power Sources*, vol. 134, pp. 262-276, 2004.
5. G. L. Plett, "Extended Kalman filtering for battery management systems of LiPB-based HEV battery packs. Part 3. State and parameter estimation," *J. Power Sources*, vol. 134, pp. 277-292, 2004.

Appendix: Kalman filter background

The EKF approach is one of the many adaptive state estimation techniques (such as Kalman filter, Luenberger's state estimator, Particle filter, Bayesian Framework etc.) that can be used for accurately estimating the inner cell SOC; and is increasingly being adopted for the LFP chemistry, in view of the difficulties presented by the chemistry as previously highlighted.
The Kalman filter [3-5] is an optimum state estimator for linear systems. However, nonlinear systems, such as LFP cells, need a linearization process at every time step to approximate the non-linear system with a linear time varying (LTV) system. This LTV is then used in the Kalman filter to produce the extended Kalman filter on the true nonlinear system. This provides an elegant method of estimating the inner 'state' of a system, based on measuring its outputs that are some function of its past and present inputs. The inner 'state' may not be directly measurable (such as SOC, hysteresis, cell relaxation dynamics etc.). The present system output can be evaluated using only the present input and present state, without storing the past inputs.

Kalman filter technique

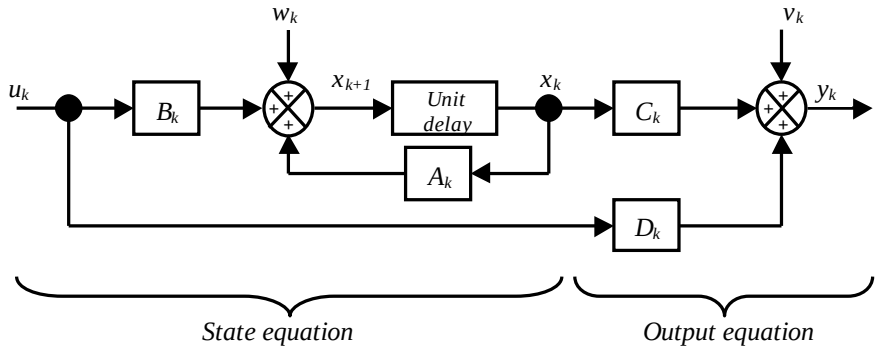

Figure 22. Block diagram of the Kalman filter in state-space form.

The general framework of the Kalman filter consists of two equations:

$$x_{k+1} = A_k x_k + B_k u_k + w_k \quad \text{(A1)}$$

$$y_k = C_k x_k + D_k u_k + v_k \quad \text{(A2)}$$

Here, x_k is the system state vector at time index *k*, and equation A1 is called the *state equation* or *process equation* as it captures the system dynamics. The input to the system is u_k which is known or can be measured. However, the measurement could result in errors, assumed to be stochastic process noise, w_k, which cannot be measured and affects the state of the system.
Equation A2 models the output of the system y_k, in terms of the input, the state vector and the noise in the measurement of the output, v_k. This equation is also called the *measurement equation* or the *output equation*.
Both w_k and v_k are assumed to be mutually uncorrelated white Gaussian random processes with zero mean and covariance matrices of known values. The equations are initialised by setting the following at k=0

$$\hat{x}_0^+ = \mathrm{E}[x_0] \quad \text{and} \quad \sum_{\tilde{x},0}^+ = \mathrm{E}[(x_0 - \hat{x}_0^+)(x_0 - \hat{x}_0^+)^T] \tag{A3}$$

where, the superscript *T* refers to the transpose of the matrix. For k=1,2,3… the following computations are made:
State estimate time update:

$$\hat{x}_k^- = A_{k-1}\hat{x}_{k-1}^+ + B_{k-1}u_{k-1} \tag{A4}$$

Error covariance time update:

$$\sum_{\tilde{x},k}^- = A_{k-1} \sum_{\tilde{x},k-1}^+ A_{k-1}^T + \sum_w \tag{A5}$$

Kalman gain matrix:

$$L_k = \sum_{\tilde{x},k}^- C_k^T \left[C_k \sum_{\tilde{x},k}^- C_k^T + \sum_v\right]^{-1} \tag{A6}$$

State estimate measurement update:

$$\hat{x}_k^+ = \hat{x}_k^- + L_k[y_k - C_k\hat{x}_k^- - D_k u_k] \tag{A7}$$

Error covariance update:

$$\sum_{\tilde{x},k}^+ = (I - L_k C_k) \sum_{\tilde{x},k}^- \tag{A8}$$

The linear discrete-time Kalman filter computes two estimates – an *a priori* estimate, $\hat{x}_k^-$, based on the prior state estimate computed in the previous iteration, $\hat{x}_{k-1}^+$. This estimate is computed *before* any system measurements are made and is denoted with a superscript "–". After the system measurements of the input u_k and output y_k , the second estimate $\hat{x}_k^+$ is more accurate and is denoted with a superscript "+". Thus, at every measurement interval, the Kalman filter first *predicts* the value of the present state, system output and error covariance: and then *corrects* the state estimate and error covariance. The prediction step is called the *time update* while the correction step is also known as the *measurement update*. The error difference between the predicted output and the actual output represents the new information and is called the *innovation process*.
The Kalman filter then optimises the minimum squared error estimate $\hat{x}_k$ of the true state x_k for the entire set of observed data {u_0, u_1…u_k} and {y_0, y_1…y_k} by solving:

$$\hat{x}_k = \arg\min \mathrm{E}[(x_k - \hat{x})^T (x_k - \hat{x})] \text{ for all inputs} \tag{A9}$$

Extended Kalman filter

As explained above, since the Kalman filter can only be used on linear systems, for nonlinear systems, the extended Kalman filter (EKF) is used by using a linearization process. The nonlinear system is depicted as:

$$x_{k+1} = f(x_k, u_k) + w_k \tag{A10}$$

$$y_k = g(x_k, u_k) + v_k \tag{A11}$$

where, w_k and v_k are white Gaussian stochastic processes with zero mean and covariance matrices Σ_w and Σ_v respectively. The functions $f(x_k, u_k)$ and $g(x_k, u_k)$ are linearized using a Taylor-series expansion, assuming that they are differentiable at all operating points.
Here, the elements of the state vector matrix are defined as:

$$\hat{A}_k = \left.\frac{\partial f(x_k,u_k)}{\partial x_k}\right|_{x_k=\hat{x}_k^+}, \quad \hat{C}_k = \left.\frac{\partial g(x_k,u_k)}{\partial x_k}\right|_{x_k=\hat{x}_k^-} \tag{A12}$$

The nonlinear state space model can be expressed as:

$$x_{k+1} \approx \hat{A}_k x_k + f(\hat{x}_k, u_k) - \hat{A}_k \hat{x}_k + w_k \quad \text{(A13)}$$

$$y_k \approx \hat{C}_k x_k + g(\hat{x}_k, u_k) - \hat{C}_k \hat{x}_k + v_k \quad \text{(A14)}$$

The terms $f(\hat{x}_k, u_k) - \hat{A}_k \hat{x}_k$ and $g(\hat{x}_k, u_k) - \hat{C}_k \hat{x}_k$ replace the terms $B_k u_k$ and $D_k u_k$ in the standard Kalman filter. The initialisation of the equations at k=0 are made as follows:

$$\hat{x}_0^+ = \mathrm{E}[x_0] \quad \text{and} \quad \sum_{\tilde{x},0}^+ = \mathrm{E}[(x_0 - \hat{x}_0^+)(x_0 - \hat{x}_0^+)^T] \quad \text{(A15)}$$

where, again the superscript *T* indicates the transpose of the matrix. For *k*=1,2,3… the following computations are made as follows:
State estimate time update:

$$\hat{x}_k^- = f(\hat{x}_{k-1}^+, u_{k-1}) \quad \text{(A16)}$$

Error covariance time update:

$$\sum_{\tilde{x},k}^- = \hat{A}_{k-1} \sum_{\tilde{x},k-1}^+ \hat{A}_{k-1}^T + \sum_w \quad \text{(A17)}$$

Kalman gain matrix:

$$L_k = \sum_{\tilde{x},k}^- \hat{C}_k^T \left[\hat{C}_k \sum_{\tilde{x},k}^- \hat{C}_k^T + \sum_v\right]^{-1} \quad \text{(A18)}$$

State estimate measurement update:

$$\hat{x}_k^+ = \hat{x}_k^- + L_k[y_k - g(\hat{x}_k^-, u_k)] \quad \text{(A19)}$$

Error covariance update:

$$\sum_{\tilde{x},k}^+ = (I - L_k \hat{C}_k) \sum_{\tilde{x},k}^- \quad \text{(A20)}$$

The above set of equations can be used to estimate the inner state vector, such as the SOC.